Weierstraß-Institut
für Angewandte Analysis und Stochastik

im Forschungsverbund Berlin e.V.

Preprint ISSN 0946 – 8633

Phase transition and hysteresis in a rechargeable lithium battery revisited

Wolfgang Dreyer[1], Miran Gaberšček[2],

Clemens Guhlke[1], Robert Huth[1] and Janko Jamnik[2]

submitted: 30th June 2009

[1] Weierstrass-Institute
for Applied Analysis
and Stochastics
Mohrenstr. 39
10117 Berlin
Germany
E-Mail: dreyer@wias-berlin.de
guhlke@wias-berlin.de
huth@wias-berlin.de

[2] Kemijski Inštitut Ljubljana Slovenija
L10 Laboratory for Materials Electrochemistry
SI-1001 Ljubljana
Hajdrihova 19
Slovenija
E-Mail: miran.gabrscek@ki.si
janko.jamnik@ki.si

No. 1425
Berlin 2009

2000 *Mathematics Subject Classification.* 74N20, 74A15, 74N05, 74B99.

Key words and phrases. lithium-ion-battery, $FePO_4$, thermodynamics, phase transitions, hysteresis, chemical potentials, surface stress, deviatoric stress, elasticity.

Edited by
Weierstraß-Institut für Angewandte Analysis und Stochastik (WIAS)
Mohrenstraße 39
10117 Berlin
Germany

Fax: + 49 30 2044975
E-Mail: preprint@wias-berlin.de
World Wide Web: http://www.wias-berlin.de/

Abstract

We revisit a model which describes the evolution of a phase transition that occurs in the cathode of a rechargeable lithium battery during the process of charging/discharging. The model is capable to simulate hysteretic behavior of the voltage - charge characteristics with two voltage plateaus.

The cathode consists of small crystalline storage particles. During discharging of the battery, the interstitial lattice sites of the particles are filled up with lithium atoms and these are released again during charging. We show within the context of a sharp interface model for a single particle of *core-shell* type that two mechanical phenomena go along with the phase transition during supply and removal of lithium. The lithium atoms need more space than is available by the interstitial lattice sites, which leads to a maximal relative change of the crystal volume of about 6%. Furthermore there is an interface between two adjacent phases that has very large curvature of the order of magnitude 10^8 m^{-1}, which evoke here a discontinuity of the normal component of the stress.

In order to simulate the dynamics within a single storage particle we establish a new initial and boundary value problem for a nonlinear PDE system that can be reduced in some limiting case to an ODE system. Furthermore we verify the common assumption of phase nucleation at the external boundary of the particle. In case of quasi static loading inner hysteresis loops in the voltage-charge plots are not contained within the setting of a core-shell model for a single storage particle. The origin of this fact is discussed in detail.

1 Introduction

The arrangement shown in Figure 1 roughly indicates the processes in a lithium battery during discharging and charging. During discharging electrons leave the anode to travel through an outer circuit. The anode is here assumed to be a metallic lithium electrode. The remaining positive lithium ions leave the anode and move through an electrolyte towards the cathode, which is the central object of the current modelling. It consists of a carbon coated single crystal $FePO_4$ with the shape of a small sphere of about 50 nm diameter. The $FePO_4$ lattice offers interstitial lattice sites that serve to store lithium atoms. When the battery is fully charged, all interstitial lattice sites are empty. During discharging the arriving lithium ions combine at the carbon coated surface of the $FePO_4$ ball with the inflowing electrons and hereafter they occupy the interstitial lattice sites. After complete discharging a maximal number of sites of the interstitial lattice is occupied by a lithium atom. During recharging of the battery the reverse process takes place.

The objective of the current study is the modelling of the loading/unloading processes of the $FePO_4$ lattice with lithium atoms. The model describes diffusion with

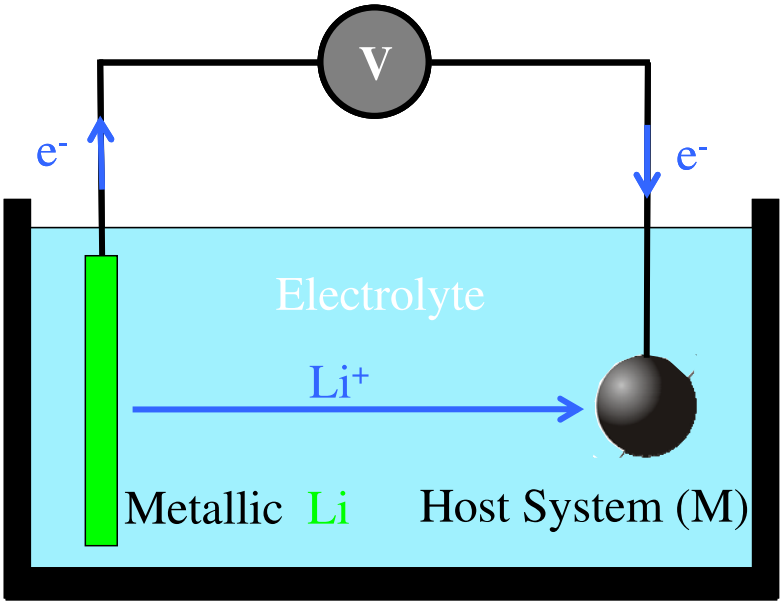

Figure 1: Basic constituents of a rechargeable lithium battery

mechanical coupling within an open system. It relies on various experimental observations and assumptions:

1. The voltage - charge plot, see Figure 2 exhibits a hysteretic behavior. The characteristics of voltage against the total charge of the battery during charging, blue arrows, is different from discharging, red arrows.

2. The lithium atoms need more space as it is offered by the interstitial lattice sites. In case of a fixed external pressure, this leads to a change of the volume of the $FePO_4$ ball up to 6% for the fully occupied interstitial lattice.

3. There is a compact region of total lithium fraction where the distribution of the lithium atoms within the $FePO_4$ ball decomposes into two phases with different local lithium fractions across the interface between the adjacent phases. Currently we assume that there is a single interface with the shape of a sphere. Thus in the 2-phase region we currently deal with an inner core and an outer shell. Furthermore we assume that the interface originates at the outer surface during loading as well as during unloading.

4. At the interface of the two phases we take surface tension into account, which is of enormous importance due to the small interfacial radius.

Further assumptions will be given later on. Here we remark that the volume change of the $FePO_4$ ball and the incorporation of surface tension at the interface lead within the model to a hysteretic behavior of the loading/unloading process.

Finally we mention a recent study, see [14], by Wagemaker, Borghols and Mulder. The authors observe a strong dependence between the maximal possible Li content and the size of the host system, and they conjecture likewise mechanical effects as

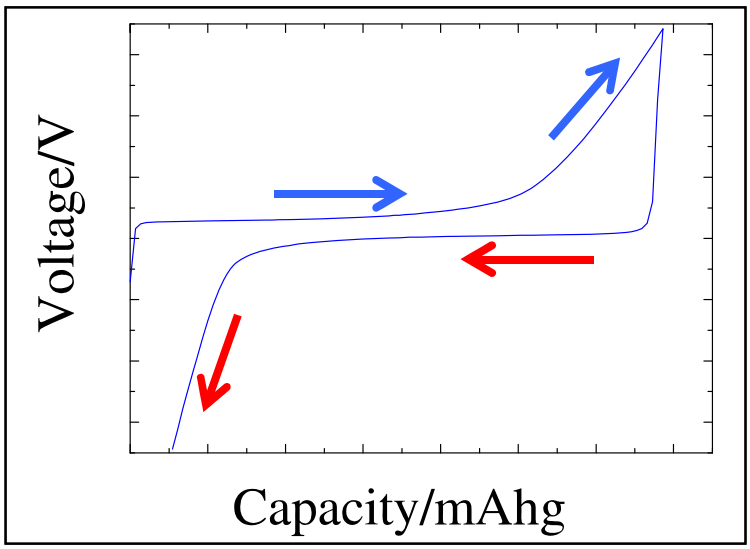

Figure 2: Typical charge and discharge curve for a LiFePO4 cathode. The voltage is plotted as a function of the total charge per mass. The charging (blue arrows) and discharging (red arrows) were performed under constant current regime. The electrode was prepared as described elsewhere [9].

the origin for this phenomenon. In fact, it is a typical feature of the mechanical boundary value problem, that the size of the considered system is of large influence.

We have organized the paper as follows:

In Chapter 2 we describe the constitution of the host system. The thermodynamic model is developed in Chapter 3 and extended in the appendix. This model relies on local conservation laws in the bulk phases, on jump conditions, i.e. Stefan conditions, across the interface and in particular on so called kinetic relations, which determine the interfacial motion and the evolution of the atomic lithium fractions on both sides of the interface. We end up with a system of nonlinear diffusion equations with mechanical coupling.

Chapter 4 considers the limiting case of infinite bulk mobility, whereby we may reduce the PDE system into an ODE system for the atomic Li fraction, the interfacial radius and the external radius of the $FePO_4$ ball as functions of time.

This ODE is analysed in Chapter 5. We determine the possible equilibria and we extract from these data the hysteretic behavior of the loading/unloading processes. Finally we examine the asymptotical evolution of the host system.

2 Constitution of the host system

The mechanical constitution of the host system from Figure 1 is described in detail by T. Maxisch and G. Ceder in [12]. It is composed of a deformable crystal lattice of

the substance $FePO_4$. The undeformed crystal has orthorhombic olivine symmetry. Furthermore there is a sublattice whose lattice sites may be empty or occupied by Li atoms. These can be supplied or removed through the external boundary, and this process is called *lithiation*. To each unit of $FePO_4$ there corresponds one single site in the sublattice. The occupation of the sublattice with Li atoms does not change the orthorhombic olivine symmetry. However, the elastic stiffness coefficients and the crystal volume change if the number of Li atoms is changed.

At room temperature there exists a region of total Li concentration where the distribution of Li atoms on the sublattice sites is realized by two coexisting phases that differ by high and small Li concentrations. Theoretical studies on the evolution of Li atoms in the host system by Han et.al [11], Srinivasan and Newman [13] and the current study rely on this phenomenon, which is experimentally investigated by Yamada et.al. [15].

Based on previous studies by Srinivasan and Newman [13] and Han et.al [11], we currently also assume that the two phases exhibit a simple morphology: They appear as an inner spherical core and an outer shell with a moving interface. However, it is important to note that in 2007 this assumed symmetry is criticized by Allen, Jow and Wolfenstine [1]. Due to some experimental hints these authors prefer a plane interface that may move in some preferred direction of the matrix lattice. For this reason we have formulated the current model in a form so that this case is included, see in particular the appendix. In other words, only the current numerical exploitation of the model relies on the spherical core assumption, so that we may follow Allen et al.'s proposal in a further study.

3 Thermodynamic description of the host system

3.1 Conservation laws of particle numbers

We consider the host system as a body Ω that may be represented by a single phase or by two coexisting phases, so that $\Omega = \Omega_- \cup \Omega_+$ as it is indicated in Figure 3. Ω_- and Ω_+ denote the inner core with radius r_{I} respectively the outer shell with radius r_0. At any time $t \geq 0$, the thermodynamic state of the body Ω is described by a certain number of variables, which may be functions of space $x = (x^i)_{i=1,2,3} = (x^1, x^2, x^3) \in \Omega$. The host system consists of three constituents: There are $FePO_4$ units (M) generating the deformable lattice, which we shall call the matrix lattice. The matrix lattice has orthorhombic symmetry in the undeformed state. Furthermore there is an interstitial sublattice, whose constituents are Li - atoms (Li) and vacancies (V). The number densities of the constituents are denoted by n_{M}, n_{Li} and n_{V}.

Among the objectives of this study is the determination of the functions

$$n_{\mathrm{M}}(t,x), \qquad n_{\mathrm{Li}}(t,x), \qquad n_{\mathrm{V}}(t,x) \quad \text{and} \quad r_{\mathrm{I}}(t), \qquad r_0(t). \tag{1}$$

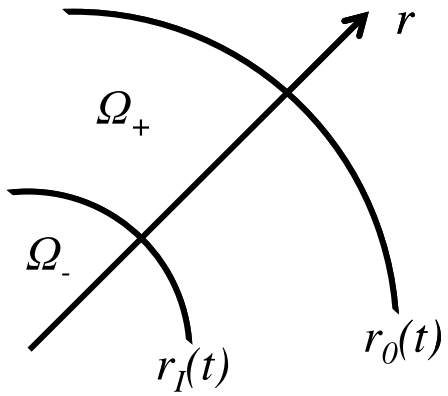

Figure 3: The 2-phase morphology of the host system

We assume that there is no diffusion on the matrix lattice, which is fully occupied by the $FePO_4$ units, so that $n_{\rm M}(t,x)$ changes exclusively due to the deformation of the lattice. On the sublattice we have diffusion, which, however, is restricted by the side condition that matrix lattice and sublattice have equal number of lattice sites, thus we have

$$n_{\rm M}(t,x) = n_{\rm Li}(t,x) + n_{\rm V}(t,x). \tag{2}$$

Next we introduce the velocities $\upsilon = (\upsilon^i)_{i=1,2,3} = (\upsilon^1, \upsilon^2, \upsilon^3)$ of the constituents by the functions

$$\upsilon_{\rm M}(t,x), \qquad \upsilon_{\rm Li}(t,x), \qquad \upsilon_{\rm V}(t,x) \tag{3}$$

According to the constraint (2) we relate the velocity of the matrix to the other velocities by

$$n_{\rm M}\upsilon_{\rm M}(t,x) = n_{\rm Li}\upsilon_{\rm Li}(t,x) + n_{\rm V}\upsilon_{\rm V}(t,x). \tag{4}$$

The constraint (4) is motivated by the conservation laws for the particle numbers, which read in regular points of Ω

$$\frac{\partial n_{\rm M}}{\partial t} + \mathrm{div}(n_{\rm M}\upsilon_{\rm M}) = 0, \quad \frac{\partial n_{\rm Li}}{\partial t} + \mathrm{div}(n_{\rm Li}\upsilon_{\rm Li}) = 0, \quad \frac{\partial n_{\rm V}}{\partial t} + \mathrm{div}(n_{\rm V}\upsilon_{\rm V}) = 0. \tag{5}$$

Due to (2) and (4) there are only two independent conservation laws, and we prefer to deal with $(5)_1$ and $(5)_2$ in the sequel.

If the state of the host system is in the 2-phase region, singular points will appear at the interface I between the adjacent phases. At I the conservation laws of particle numbers assume the form

$$-w^\nu[[n_{\rm M}]] + [[n_{\rm M}\upsilon^\nu_{\rm M}]] = 0, \quad -w^\nu[[n_{\rm Li}]] + [[n_{\rm Li}\upsilon^\nu_{\rm Li}]] = 0, \quad -w^\nu[[n_{\rm V}]] + [[n_{\rm V}\upsilon^\nu_{\rm V}]] = 0. \tag{6}$$

Herein w^ν denotes the normal speed of the interface and ν is the normal vector, which points into the + region. The double bracket gives the difference of a quantity that suffers a discontinuity at the interface: $[[\psi]] \equiv \psi_+ - \psi_-$.

We conclude that the atomic fluxes

$$\dot{\mathcal{N}}_{\mathrm{M}} \equiv -n_{\mathrm{M}}(\upsilon_{\mathrm{M}}^{\nu} - w^{\nu}), \quad \dot{\mathcal{N}}_{\mathrm{Li}} \equiv -n_{\mathrm{Li}}(\upsilon_{\mathrm{Li}}^{\nu} - w^{\nu}) \quad \text{and} \quad \dot{\mathcal{N}}_{V} \equiv -n_{\mathrm{V}}(\upsilon_{\mathrm{V}}^{\nu} - w^{\nu}) \tag{7}$$

are continuous across the interface, i.e.

$$\dot{\mathcal{N}}_{\mathrm{M}}^{+} = \dot{\mathcal{N}}_{\mathrm{M}}^{-}, \quad \dot{\mathcal{N}}_{\mathrm{Li}}^{+} = \dot{\mathcal{N}}_{\mathrm{Li}}^{-}, \quad \text{and} \quad \dot{\mathcal{N}}_{\mathrm{V}}^{+} = \dot{\mathcal{N}}_{\mathrm{V}}^{-}. \tag{8}$$

In the considered case of spherical morphology, the interface is completely described by its time dependent radius $r_{\mathrm{I}}(t)$. In this case we have in polar coordinates $\nu = (1, 0, 0)$ and $w^{\nu} = \dot{r}_{\mathrm{I}}(t)$. Likewise in the bulk, we take $(8)_1$ and $(8)_2$ as the two independent conservation laws for $x \in I$.

The quantities that appear in the conservation laws of particle numbers can be combined to define further quantities that are needed for the description of the thermodynamic state of the host system. Among these are the mass density ρ and the barycentric velocity υ, which are defined by

$$\rho \equiv m_{\mathrm{Li}} n_{\mathrm{Li}} + m_{\mathrm{M}} n_{\mathrm{M}} \quad \text{and} \quad \rho\upsilon \equiv m_{\mathrm{Li}} n_{\mathrm{Li}} \upsilon_{\mathrm{Li}} + m_{\mathrm{M}} n_{\mathrm{M}} \upsilon_{\mathrm{M}}, \tag{9}$$

where m_{M} and m_{Li} denote the atomic masses of $FePO_4$ and Li. Note that the vacancies do not contribute to mass density and barycentric velocity .

A linear combination of the conservations laws for particle numbers imply the conservation laws for the total mass, viz.

$$\frac{\partial \rho}{\partial t} + \operatorname{div}(\rho\upsilon) = 0 \quad \text{for} \quad x \in \Omega_{+/-} \quad \text{and} \quad -w^{\nu}[[\rho]] + [[\rho\upsilon^{\nu}]] = 0 \quad \text{for} \quad x \in I. \tag{10}$$

Next we introduce the atomic fraction of Li, y, and the diffusion fluxes with respect to the velocity υ_{M} of the crystal lattice, $j_{\mathrm{Li}} = (j_{\mathrm{Li}}^{i})_{i=1,2,3}$ and $j_{\mathrm{V}} = (j_{\mathrm{V}}^{i})_{i=1,2,3}$:

$$y \equiv \frac{n_{\mathrm{Li}}}{n_{\mathrm{M}}}, \quad j_{\mathrm{Li}} \equiv n_{\mathrm{Li}}(\upsilon_{\mathrm{Li}} - \upsilon_{\mathrm{M}}), \quad j_{\mathrm{V}} \equiv n_{\mathrm{V}}(\upsilon_{\mathrm{V}} - \upsilon_{\mathrm{M}}). \tag{11}$$

Diffusion fluxes with respect to the barycentric velocity υ are also important, $f_{\mathrm{Li}} = (f_{\mathrm{Li}}^{i})_{i=1,2,3}$, $f_{\mathrm{V}} = (f_{\mathrm{V}}^{i})_{i=1,2,3}$ and $f_{\mathrm{M}} = (f_{\mathrm{M}}^{i})_{i=1,2,3}$:

$$f_{\mathrm{Li}} \equiv n_{\mathrm{Li}}(\upsilon_{\mathrm{Li}} - \upsilon), \quad f_{\mathrm{V}} \equiv n_{\mathrm{V}}(\upsilon_{\mathrm{V}} - \upsilon) \quad \text{and} \quad f_{\mathrm{M}} \equiv n_{\mathrm{M}}(\upsilon_{\mathrm{M}} - \upsilon). \tag{12}$$

Finally we list several identities between the various diffusion fluxes. They read

$$j_{\mathrm{Li}} + j_{\mathrm{V}} = 0, \quad m_{\mathrm{Li}} f_{\mathrm{Li}} + m_{\mathrm{M}} f_{\mathrm{M}} = 0, \quad f_{\mathrm{Li}} = j_{\mathrm{Li}} + y f_{\mathrm{M}}, \quad f_{\mathrm{V}} = j_{\mathrm{V}} + (1 - y) f_{\mathrm{M}}, \tag{13}$$

and at the interface we have

$$m_{\mathrm{Li}} \dot{\mathcal{N}}_{\mathrm{Li}} + m_{\mathrm{M}} \dot{\mathcal{N}}_{\mathrm{M}} = -\rho(\upsilon^{\nu} - w^{\nu}). \tag{14}$$

3.2 Conservation law of momentum

The conservation law of momentum determines the motion of the matrix lattice, i.e. the displacement $u = (u^i)_{i=1,2,3} = (u^1, u^2, u^3)$. If we ignore elastic waves in the matrix lattice, this conservation law reduces to a quasi-static force balance, which reads in regular points in Ω

$$\text{div } \sigma = 0. \tag{15}$$

The newly introduced quantity $\sigma = (\sigma^{ij})_{i,j=1,2,3}$ is the Cauchy stress tensor with $\sigma^{ij} = \sigma^{ji}$. The detailed description of motion, strain and stresses will be given in the Appendix, because here we apply a simplified mechanical model that ignores (i) the orthorhombic symmetry and (ii) the deviatoric stresses so that the stress tensor reduces to a pressure p: $\sigma^{ij} = -p\delta^{ij}$.

The quasi-static momentum balance at the interface I is given by

$$[[\sigma^{ij}]]\nu^j = -2\gamma k_M \nu^i, \quad \text{respectively for the special case at hand} \quad [[p]] = -\frac{2\gamma}{r_{\mathrm{I}}}. \tag{16}$$

$\gamma > 0$ is the surface tension and k_M denotes the mean curvature, which reads in polar coordinates for a sphere: $k_M = -1/r_{\mathrm{I}}$.

3.3 Constitutive Model, Part 1: Some pieces of the second law of thermodynamics

In this and the following sections we rely on the recent study by Dreyer et.al. [2] to show that the knowledge of the free energy is sufficient in order to give all constitutive quantities as functions of the variables. Here we start with the assumption that the specific free energy, ψ, is given by the general representations

$$\psi = \hat{\psi}(T, n_{\mathrm{Li}}, n_{\mathrm{V}}) = \tilde{\psi}(T, y, \rho). \tag{17}$$

The both functions $\hat{\psi}$ and $\tilde{\psi}$ are related to each other in a simple manner by means of the transformation

$$y = \frac{n_{\mathrm{Li}}}{n_{\mathrm{Li}} + n_{\mathrm{V}}} \quad \text{and} \quad \rho = (n_{\mathrm{Li}} + n_{\mathrm{V}})m(y) \quad \text{with} \quad m(y) \equiv m_{\mathrm{M}} + m_{\mathrm{Li}} y. \tag{18}$$

In the following, the function $\hat{\psi}$ will be used to calculate the chemical potentials μ_{Li} and μ_{V} whereas $\tilde{\psi}$ gives the pressure p. According to the 2^{nd} law of thermodynamics we have, see [2] for details,

$$\mu_{\mathrm{Li}} = \frac{\partial \rho\hat{\psi}}{\partial n_{\mathrm{Li}}}, \quad \mu_{\mathrm{V}} = \frac{\partial \rho\hat{\psi}}{\partial n_{\mathrm{V}}}, \quad p = \rho^2 \frac{\partial \tilde{\psi}}{\partial \rho}, \quad \rho\psi + p = \mu_{\mathrm{Li}} n_{\mathrm{Li}} + \mu_{\mathrm{V}} n_{\mathrm{V}}. \tag{19}$$

The equations $(19)_1$ to $(19)_3$ give some parts of the Gibbs equation and $(19)_4$ is called Gibbs-Duhem equation. The explicit form of the functions $\hat{\psi}$ and $\tilde{\psi}$ will be given and exploited in the next Section.

A further content of the 2nd law of thermodynamics is the entropy inequality, which identifies on its left hand side the entropy production in the two bulk phases. It reads

$$-f_{\mathrm{Li}}\nabla\mu_{\mathrm{Li}} - f_{\mathrm{V}}\nabla\mu_{\mathrm{V}} = -f_{\mathrm{Li}}\nabla(\mu_{\mathrm{Li}} - \frac{m_{\mathrm{Li}}+m_{\mathrm{M}}}{m_{\mathrm{M}}}\mu_{\mathrm{V}}) \geq 0. \tag{20}$$

The equality sign holds in equilibrium, where the entropy production assumes its minimum value zero. In non-equilibrium the production of entropy must be positive. Thus in equilibrium we have $f_{\mathrm{Li}} = 0$ and $\nabla(\mu_{\mathrm{Li}} - (m_{\mathrm{Li}}+m_{\mathrm{M}})/m_{\mathrm{M}}\ \mu_{\mathrm{V}}) = 0$.

The most simple possibility to satisfy the entropy inequality in non-equilibrium is given by Fick's law

$$f_{\mathrm{Li}} = -M_B(T,y)\nabla(\mu_{\mathrm{Li}} - \frac{m_{\mathrm{Li}}+m_{\mathrm{M}}}{m_{\mathrm{M}}}\mu_{\mathrm{V}}), \tag{21}$$

where the bulk mobility satisfies $M_B(T,y) > 0$.

Note that the entropy inequality holds point-wise, thus there is also an inequality at the interface I, viz.

$$-\rho(\upsilon^\nu - w^\nu)[[\psi + \frac{1}{2}(\upsilon - w)^2]] + [[\sigma^{ij}(\upsilon^i - w^i)]]\nu^j - [[\mu_{\mathrm{Li}}f^\nu_{\mathrm{Li}} + \mu_{\mathrm{V}}f^\nu_{\mathrm{V}}]] \geq 0. \tag{22}$$

The derivation of the entropy inequalities (20) and (22) are found to be in [4] and [3]. In particular details concerning the treatment of vacancies and side conditions are given there.

The interfacial entropy production will be used to formulate relations that are similar to Fick's law in the bulk phases. To this end we bring the left hand side of (22) by means of $\sigma^{ij} = -p\delta^{ij}$, the flux definitions (11), (12) and (7), the conservation laws (8), the Gibbs-Duhem relation $(19)_4$ and the identities (13) and (14) into a more appropriate form:

$$\dot{\mathcal{N}}_{\mathrm{Li}}[[\mu_{\mathrm{Li}} - \mu_{\mathrm{V}} + \frac{m_{\mathrm{Li}}}{2}(\upsilon - w)^2]] + \dot{\mathcal{N}}_{\mathrm{M}}[[\mu_{\mathrm{V}} + \frac{m_{\mathrm{M}}}{2}(\upsilon - w)^2]] \geq 0. \tag{23}$$

Note the similarity between (20) and (23). In any case the entropy production is a sum of products *flux* $\times$ *driving force*. In (20) the flux is the diffusion flux of Li and the driving force has to be identified with the gradient of a chemical potential difference. At the interface two products contribute to the entropy production: The flux of the first contribution is the atomic Li flux across the interface and the jump of the chemical potential difference plus a kinetic contribution is the driving force. The flux of the second product is identified as the atomic $FePO_4$ flux and the driving force is the jump consisting of the chemical potential of the vacancies plus a kinetic contribution. The both kinetic contributions are often small in comparison with the chemical potentials.

The equality sign of (23) holds in equilibrium and in non-equilibrium the interfacial entropy production must be positive. Thus in equilibrium we have $\dot{\mathcal{N}}_{\mathrm{Li}} = 0$ and $\dot{\mathcal{N}}_{\mathrm{M}} = 0$, and the possible equilibria are determined by

$$[[\mu_{\mathrm{Li}} - \mu_{\mathrm{V}}]] = 0 \quad \text{and} \quad [[\mu_{\mathrm{V}}]] = 0. \tag{24}$$

In an analogous manner to the bulk, the simplest possibility to satisfy the interfacial entropy production in equilibrium as well as in non-equilibrium is given by the ansatz

$$\dot{\mathcal{N}}_{\mathrm{Li}} = M_{\mathrm{I}}^{Li}[[\mu_{\mathrm{Li}} - \mu_{\mathrm{V}} + \frac{m_{\mathrm{Li}}}{2}(v-w)^2]], \quad \text{and} \quad \dot{\mathcal{N}}_{\mathrm{M}} = M_{\mathrm{I}}^{M}[[\mu_{\mathrm{V}} + \frac{m_{\mathrm{M}}}{2}(v-w)^2]]. \tag{25}$$

Thus there are two positive mobilities at the interface, viz. M_{I}^{Li} and M_{I}^{M}.

We may conclude from the results of this section that if we were to know the free energy density, we could calculate all the other constitutive quantities. However, the bulk mobility and the two interfacial mobilities must be determined either by statistical thermodynamics or by experiments.

3.4 Constitutive law, Part2: Explicit forms of the pressure, free energy density and chemical potentials

The strategy to determine the specific free energy, i.e. the two functions $\hat{\psi}(T, n_{\mathrm{Li}}, n_{\mathrm{V}})$ and $\tilde{\psi}(T, y, \rho)$, is as follows: At first we use $(19)_3$ to determine the ρ dependence of the function $\tilde{\psi}$, which is given by the pressure. Therefore we start with a constitutive law that relates the pressure to the volume change of the matrix lattice. We assume

$$p = \bar{p} + K(\frac{n_{\mathrm{M}}}{\bar{n}_{\mathrm{M}}} - h(y)) \quad \text{with} \quad h(y) = \frac{1}{1+y\delta}\ . \tag{26}$$

Here $\bar{n}_{\mathrm{M}}$ denotes the particle density of $FePO_4$ in the undeformed reference state of the matrix lattice. The bulk modulus is denoted by K. According to [12], K depends on the Li fraction y, but we ignore that fact in the simplified model. The function $h(y)$ describes the phenomenon that Li atoms need more space than the vacancies. If $\delta = 0$ we were to have $n_{\mathrm{M}} = \bar{n}_{\mathrm{M}}$ at $p = \bar{p}$. However, there is a volumetric expansion $(V - \bar{V})/\bar{V}$ of the host system if the Li fraction changes from 0 to 1. We denote its maximum for $y = 1$ by $\delta \equiv (V_{\max} - \bar{V})/\bar{V}$, which is about 0.06. For other values of y we simply interpolate and write $(V - \bar{V})/\bar{V} = y\delta$. The volume expansion is measured at the reference pressure, where we have $n_{\mathrm{M}}/\bar{n}_{\mathrm{M}} = h(y)$, on the other hand $n_{\mathrm{M}}/\bar{n}_{\mathrm{M}} = \bar{V}/V$, therefore we obtain $h(y)$ as it is given by $(26)_2$.

Next we apply $(19)_3$ to calculate the mechanical part of the free energy from the pressure. Since the derivative of the function $\tilde{\psi}$ depends on the variables y and ρ, we represent p in the same variables, and we integrate

$$\frac{\partial \tilde{\psi}}{\partial \rho} = \frac{p}{\rho^2} = \frac{\bar{p} - Kh(y)}{\rho^2} + \frac{K}{\bar{n}_{\mathrm{M}} m(y)}\frac{1}{\rho}. \tag{27}$$

We obtain

$$\rho\tilde{\psi}(T, y, \rho) = (\bar{p} - Kh(y))(\frac{\rho}{\bar{n}_{\mathrm{M}} m(y) h(y)} - 1) + K\frac{\rho}{\bar{n}_{\mathrm{M}} m(y)} \log(\frac{\rho}{\bar{n}_{\mathrm{M}} m(y) h(y)}) + \frac{\rho}{m(y)} C(T, y). \tag{28}$$

We have chosen the integration constant so that the remaining unknown function $C(T, y)$ can be identified with the chemical part of the free energy density, which is defined by

$$C(T, y) \equiv \tilde{\psi}^{\text{chem}}(T, y) \equiv \tilde{\psi}(T, y, \bar{n}_{\text{M}} m(y) h(y)). \tag{29}$$

The definition of the chemical part relies on the fact that this part is determined at constant reference pressure, which is guaranteed by the definition (29). We now can also define the mechanical part of the free energy density by

$$\rho\psi^{\text{mech}} \equiv \rho\psi - \rho\psi^{\text{chem}}, \tag{30}$$

and we conclude that the first two terms on the right hand side of (28) give $\rho\psi^{\text{mech}}$.

The motivation of that decomposition relies on the fact, that our knowledge on the two contributions to the free energy originates from different sources. The chemical part can be calculated within statistical thermodynamics, and the simplest model that is capable to exhibit two coexisting phases is given by, see also the phase field approach by Han et. al. [11] where the same function is used,

$$\rho\psi^{\text{chem}} = n_{\text{M}}\Omega \left(y(1-y) + \frac{kT}{\Omega}(y\log(y) + (1-y)\log(1-y)\right) \equiv n_{\text{M}}\Omega f(y). \tag{31}$$

The first term gives an energetic contribution whose strength is controlled by the constant $\Omega > 0$, whereas the second contribution is purely entropic. k denotes the Boltzmann constant. Note that the positivity of Ω may lead to a non-convex function, which is necessary to obtain two coexisting phases.

Thus the free energy density for the host system can be written as

$$\rho\psi = \Omega n_{\text{M}} f(y) + (\bar{p} - Kh(y))(\frac{n_{\text{M}}}{\bar{n}_{\text{M}} h(y)} - 1) + K\frac{n_{\text{M}}}{\bar{n}_{\text{M}}}\log(\frac{n_{\text{M}}}{\bar{n}_{\text{M}} h(y)}) \tag{32}$$

Next we calculate the chemical potentials. According to $(19)_1$ and $(19)_2$ we need the identities

$$\frac{\partial n_{\text{M}}}{\partial n_{\text{Li}}} = 1, \quad \frac{\partial n_{\text{M}}}{\partial n_{\text{V}}} = 1, \quad \frac{\partial y}{\partial n_{\text{Li}}} = \frac{1-y}{n_{\text{M}}}, \quad \frac{\partial y}{\partial n_{\text{V}}} = -\frac{y}{n_{\text{M}}}\ . \tag{33}$$

We obtain for Li

$$\begin{aligned}\frac{1}{\Omega}\mu_{\text{Li}} = f + (1-y)f' + \\ a_1\left(\log(\frac{n_{\text{M}}}{\bar{n}_{\text{M}} h}) - \frac{h'}{h}(1 - \frac{\bar{n}_{\text{M}} h}{n_{\text{M}}})(1-y)\right) + a_2\left(1 - \frac{h'}{h}(1-y)\right)\frac{1}{h},\end{aligned} \tag{34}$$

and for the vacancies

$$\frac{1}{\Omega}\mu_{\text{V}} = f - yf' + a_1\left(\log(\frac{n_{\text{M}}}{\bar{n}_{\text{M}} h}) + \frac{h'}{h}(1 - \frac{\bar{n}_{\text{M}} h}{n_{\text{M}}})y\right) + a_2\left(1 + \frac{h'}{h}y\right)\frac{1}{h}. \tag{35}$$

The newly introduced constants $a_1 = K/\bar{n}_{\text{M}}\Omega$ and $a_2 = \bar{p}/\bar{n}_{\text{M}}\Omega$ control the strength of mechanical in comparison to chemical driving forces.

4 The model for infinite bulk diffusivity and spherical symmetry

In this section we exploit the thermodynamic model for the host system under some assumptions that will drastically simplify the analysis. The general case will be treated in a forthcoming study.

4.1 Simplifying assumptions

Recall that the model contains three inherent time scales, and a fourth time scale is given by the boundary conditions. These scales can be extracted from the mobility in the bulk, M_{B}, the mobilities for interfacial kinetics, M^I_{Li} and M^I_{M}, and the speed of supply and removal of Li atoms at the outer boundary. Relying on data found in [11], we now assume that the fastest of these processes is diffusion in the bulk, and we consider the limiting case of infinite bulk mobility. In other words: For finite diffusion flux and infinite bulk mobility, the chemical potentials and thus the number densities of the constituents become homogeneous within the two phases, because Fick's law (21), viz. $f_{\mathrm{Li}} = -M_{\mathrm{B}} \nabla(\mu_{\mathrm{Li}} - (m_{\mathrm{Li}} + m_{\mathrm{M}})/m_{\mathrm{M}}\ \mu_{\mathrm{V}})$, assumes the form $f_{\mathrm{Li}} = -\infty \times 0$ and thus cannot be used anymore to determine the diffusion flux in this limiting case. In fact we shall see that for infinite bulk mobility f_{Li} follows from the local conservation law for the Li content.

In Section 3.4 we have already ignored the orthorhombic symmetry of the matrix lattice and the deviatoric stress components, so that the constitutive law (26) for the pressure is sufficient to describe the deformation of the lattice.

A further assumption concerns the geometric shape of the host system and of the interface I. We assume that the host system is a sphere with outer time dependent radius $r_0(t)$, and the morphology of the distribution of the two phases is an inner core Ω_- with interfacial radius r_{I} and an outer shell Ω_+. It is important to note that this assumption has been criticized by Allen et. al., see [1], and we shall devote a further study to their reasonings.

Finally we have to fix the location $r_{\mathrm{I}}(t_0)$ where the interface starts when we enter into the 2-phase region. Loading and unloading of the host system with Li atoms happens at the outer boundary. Despite the idealized assumption of homogeneity of the densities in bulk, it is obvious that if we reach the 2-phase region by supply of Li at r_0, the Li fraction will be slightly larger here than in the interior, so that the interface will start at the outer boundary for the loading process. On the other, the interface will also start at the outer boundary if we approach the 2-phase region during unloading of Li, because in that case the Li fraction at r_0 will obviously be slightly smaller than in the interior.

4.2 Conservation of particle numbers

The total number N_{M} of $FePO_4$ particles is conserved, and we can formulate its global conservation law $N_{\mathrm{M}} = N_{\mathrm{M}}^- + N_{\mathrm{M}}^+$, which reads more explicitly for the simplified case at hand

$$\bar{n}_{\mathrm{M}} \bar{r}_0^3 = n_{\mathrm{M}}^- r_{\mathrm{I}}^3 + n_{\mathrm{M}}^+ (r_0^3 - r_{\mathrm{I}}^3). \tag{36}$$

Recall that $\bar{n}_{\mathrm{M}}$ is the density of $FePO_4$ particles in the deformation free reference state, i.e. $y = 0$ and $p = \bar{p}$. The outer radius of the host system in this state is denoted by $\bar{r}_0$.

The host system is an open system for Li, therefore the ratio q of the total number of Li atoms and the total number of intersitial lattice sittes, i.e. $q(t) = N_{\mathrm{Li}}(t)/N_{\mathrm{M}}$, is a function of time and we have

$$q = \frac{n_{\mathrm{Li}}^- r_{\mathrm{I}}^3 + n_{\mathrm{Li}}^+ (r_0^3 - r_{\mathrm{I}}^3)}{\bar{n}_{\mathrm{M}} \bar{r}_0^3} \ . \tag{37}$$

4.3 The mechanical problem

The mechanical problem which is formulated in Section 3.2 reads in radial coordinates

$$\frac{\partial p}{\partial r} = 0 \quad \text{for} \quad r \in \Omega_{+/-}(t) \quad \text{and} \quad p^- - p^+ = \frac{2\gamma}{r_{\mathrm{I}}} \quad \text{for} \quad r = r_{\mathrm{I}}(t). \tag{38}$$

From $(38)_1$ we conclude

$$p = p^+(t) \quad \text{for} \quad r \in \Omega_+(t) \quad \text{and} \quad p = p^-(t) \quad \text{for} \quad r \in \Omega_-(t). \tag{39}$$

There are two cases possible that lead to different boundary conditions at the outer boundary $r = r_0(t)$.

Case 1: The outer pressure p_0 is fixed, i.e. $p^+ = p_0$. In that case the outer radius r_0 changes in fact with time and must be calculated from the conservation law (36).

Case 2: The external radius r_0 is fixed, i.e. $r = r_0$. In that case the pressure $p^+ = p_0(t)$ changes with time and must be calculated from the constitutive law (26).

At first we exploit the pressure controlled Case 1. We insert the constitutive law (26) into $p^+ = p_0$ and into the interfacial condition $(38)_2$ to obtain

$$n_{\mathrm{M}}^+ = \bar{n}_{\mathrm{M}} (h(y^+) + \frac{1}{K}(p_0 - \bar{p})) \quad \text{and} \quad n_{\mathrm{M}}^- = \bar{n}_{\mathrm{M}} (h(y^-) + \frac{1}{K}(p_0 - \bar{p} + \frac{2\gamma}{r_{\mathrm{I}}})). \tag{40}$$

Finally we solve the conservation law (36) for $r_0(t)$,

$$r_0^3 = \frac{1}{n_{\mathrm{M}}^+} (\bar{n}_{\mathrm{M}} \bar{r}_0^3 + (n_{\mathrm{M}}^+ - n_{\mathrm{M}}^-) r_{\mathrm{I}}^3). \tag{41}$$

Thus we are able to eliminate n_{M}^{+} and n_{M}^{-} in the chemical potentials, see (34) and (35), and we end up with chemical potentials that depend on the Li fractions y^{-}, y^{+} and on the interfacial radius r_{I}.

In an analogous manner we treat the volume controlled Case 2. Here the resulting density of the matrix constituent reads in Ω_{+}

$$n_{\mathrm{M}}^{+} = \frac{\bar{n}_{\mathrm{M}}\bar{r}_0^3}{r_0^3}(1 + (h(y^{+}) - h(y^{-}))(\frac{r_{\mathrm{I}}}{\bar{r}_0})^3 - \frac{2\gamma}{K}(\frac{r_{\mathrm{I}}}{\bar{r}_0})^2), \tag{42}$$

and in Ω_{-} we have

$$n_{\mathrm{M}}^{-} = \frac{\bar{n}_{\mathrm{M}}\bar{r}_0^3}{r_0^3}(1 + (h(y^{+}) - h(y^{-}))((\frac{r_0}{\bar{r}_0})^3 - (\frac{r_{\mathrm{I}}}{\bar{r}_0})^3) + \frac{2\gamma}{K}\frac{1}{r_{\mathrm{I}}}((\frac{r_0}{\bar{r}_0})^3 - (\frac{r_{\mathrm{I}}}{\bar{r}_0})^3)). \tag{43}$$

For fixed r_0, the pressure p_0 depends on time, and this dependence is obviously given by

$$p_0 = \bar{p} + K(\frac{n_{\mathrm{M}}^{+}(t)}{\bar{n}_{\mathrm{M}}} - h(y^{+}(t))). \tag{44}$$

Note that the possibility to treat the mechanical problem independent of the diffusion problem is an extraordinary case, which is meet here because we have ignored deviatoric stresses, so that the stress tensor reduces to a pressure. In the general case diffusion and mechanics must be solved simultaneously.

4.4 Evolution equations

Finally we exploit the evolution equations (25) for spherical symmetry. In this case it is easy to show by means of the definitions (7) that we have

$$\dot{\mathcal{N}}_{\mathrm{Li}}^{-} = \frac{1}{4\pi r_{\mathrm{I}}^2}\frac{d}{dt}(n_{\mathrm{M}}^{-}y^{-}\frac{4\pi}{3}r_{\mathrm{I}}^3) \quad \text{and} \quad \dot{\mathcal{N}}_{\mathrm{M}}^{-} = \frac{1}{4\pi r_{\mathrm{I}}^2}\frac{d}{dt}(n_{\mathrm{M}}^{-}\frac{4\pi}{3}r_{\mathrm{I}}^3). \tag{45}$$

We insert these identities into the left hand sides of the kinetic relations (25) and obtain

$$\frac{r_{\mathrm{I}}}{3}\frac{d}{dt}(n_{\mathrm{M}}^{-}y^{-}) + n_{\mathrm{M}}^{-}y^{-}\frac{dr_{\mathrm{I}}}{dt} = M_{\mathrm{I}}^{\mathrm{Li}}[[\mu_{\mathrm{Li}} - \mu_{\mathrm{V}} + \frac{m_{\mathrm{Li}}}{2}(v - w)^2]], \tag{46}$$

$$\frac{r_{\mathrm{I}}}{3}\frac{dn_{\mathrm{M}}^{-}}{dt} + n_{\mathrm{M}}^{-}\frac{dr_{\mathrm{I}}}{dt} = M_{\mathrm{I}}^{\mathrm{M}}[[\mu_{\mathrm{V}} + \frac{m_{\mathrm{M}}}{2}(v - w)^2]]. \tag{47}$$

These equations and the conditions (36),(37) determine the evolution of the interface radius r_{I} and of the atomic Li fractions $y^{+/-}$. To this end, however, one has to eliminate $n_{\mathrm{M}}^{+/-}$ by means of (40) for fixed external pressure p_0 or with (42), (43) for fixed external radius r_0.

4.5 Dimensionless quantities

We introduce dimensionless quantities by means of the time scale of the external flux, t_0, and the radius $\bar{r}_0$ of the host system for $y = 0$,

$$\tau \equiv \frac{t}{t_0}, \quad \xi_{\mathrm{I}} \equiv \frac{r_{\mathrm{I}}}{\bar{r}_0}, \quad \xi_0 \equiv \frac{r_0}{\bar{r}_0}. \tag{48}$$

The dimensionless internal time scales are defined by

$$\tau_{\mathrm{Li}} \equiv \frac{\bar{n}_{\mathrm{M}}\bar{r}_0}{M^{\mathrm{I}}_{\mathrm{Li}}\Omega}, \quad \tau_{\mathrm{M}} \equiv \frac{\bar{n}_{\mathrm{M}}\bar{r}_0}{M^{\mathrm{I}}_{\mathrm{M}}\Omega}. \tag{49}$$

Furthermore we define dimensionless versions of the density of the matrix lattice, the diffusion flux, chemical potentials, the surface tension, the bulk modulus, and the external pressure, viz.

$$\nu \equiv \frac{n_{\mathrm{M}}}{\bar{n}_{\mathrm{M}}}, \quad J \equiv \frac{\bar{r}_0\bar{n}_{\mathrm{M}}}{t_0}j, \quad \tilde{\mu} \equiv \frac{\mu}{\Omega}, \quad \tilde{\gamma} \equiv \frac{\gamma}{\bar{p}\bar{r}_0}, \quad \tilde{K} \equiv \frac{K}{\bar{p}}, \quad P \equiv \frac{p_0}{\bar{p}} - 1. \tag{50}$$

4.6 Summary

For fixed external pressure P we now give the explicit evolution system and initial and boundary data in dimensionless quantities for the three variables $y^{+/-}$ and ξ_{I}. The case of fixed external radius ξ_0 will be exploited in a further paper.

The evolution equations rely on the ODE system (46) and (47). The appearing kinetic energies are small for the case at hand and thus can be ignored. After some simple rearrangements we have

$$\frac{1}{3}\nu^-\xi_{\mathrm{I}}\frac{dy^-}{dt} = \frac{1}{\tau_{\mathrm{Li}}}(\mu^+ - \mu^-) - y^-\frac{1}{\tau_{\mathrm{M}}}(\mu^+_{\mathrm{V}} - \mu^-_{\mathrm{V}}), \tag{51}$$

$$\nu^-(\nu^- - \frac{1}{3}\frac{2\gamma}{K}\frac{1}{\xi_{\mathrm{I}}})\frac{d\xi_{\mathrm{I}}}{dt} = \frac{-h'(y^-)}{\tau_{\mathrm{Li}}}(\mu^+ - \mu^-) + (\nu^- + y^-h'(y^-))\frac{1}{\tau_{\mathrm{M}}}(\mu^+_{\mathrm{V}} - \mu^-_{\mathrm{V}}). \tag{52}$$

The conditions (36), (37) serve to determine y^+ according to

$$y^+ = \frac{q - y^-\nu^-\xi_{\mathrm{I}}^3}{1 - \nu^-\xi_{\mathrm{I}}^3}\ , \tag{53}$$

where the source function $q(\tau)$ is the ratio of the total number of Li atoms and the total number of interstitial lattice sites. The solution of the mechanical problem provides the dimensionless densities of the matrix particles in $\Omega_{+/-}$

$$\nu^+ = h(y^+) + \frac{1}{K}P \quad \text{and} \quad \nu^- = h(y^-) + \frac{1}{K}(P + \frac{2\gamma}{\xi_{\mathrm{I}}}), \tag{54}$$

and the dimensionless external radius

$$\xi_0^3 = \frac{1}{\nu^+}(1 + (\nu^+ - \nu^-)\xi_{\mathrm{I}}^3), \tag{55}$$

which changes with time for fixed external pressure.

For completeness we also write down the density of matrix particles for the case of fixed volume. Recall that we shall not exploit this case here.

$$\nu^+ = (1 + (h(y^+) - h(y^-))\xi_{\rm I}^3 - \frac{2\gamma}{K}\xi_{\rm I}^2, \tag{56}$$

$$\nu^- = (1 + (h(y^+) - h(y^-))(\xi_0^3 - \xi_{\rm I}^3) + \frac{2\gamma}{K}\frac{1}{\xi_{\rm I}}(\xi_0^3 - \xi_{\rm I}^3). \tag{57}$$

Finally we give the chemical potentials $\mu \equiv \mu_{\rm Li} - \mu_{\rm V}$ and $\mu_{\rm V}$ in terms of the dimensionless variables:

$$\mu = f'(y) - a_1\frac{h'(y)}{h(y)}(1 - \frac{h(y)}{\nu}) - a_2\frac{h'(y)}{h(y)^2}, \tag{58}$$

$$\mu_{\rm V} = f(y) - yf'(y) + a_1\left(\log(\frac{\nu}{h(y)}) + \frac{h'(y)}{h(y)}(1 - \frac{h(y)}{\nu})y\right) + a_2\left(1 + \frac{h'(y)}{h(y)}y\right)\frac{1}{h(y)}, \tag{59}$$

The functions h and ν account for the mechanical contributions to the chemical potentials. Note that from (54) we have different representations for ν in $\Omega_{+/-}$, viz. $\nu^+(P, y^+)$ and $\nu^-(P, \xi_{\rm I}, y^-)$. Accordingly there result different functions that represent the chemical potentials in the two phases. For the case of fixed external pressure these are written as $\mu^+(P, y^+)$, $\mu^-(P, \xi_{\rm I}, y^+)$ and $\mu_{\rm V}^+(P, y^+)$, $\mu_{\rm V}^-(P, \xi_{\rm I}, y^-)$. On the other hand, if we consider a fixed external radius ξ_0, we have $\nu^{+/-}(\xi_0, \xi_{\rm I}, y^+, y^-)$, i.e. both Li fractions appear in ν^+ as well as in ν^- and thus the chemical potential functions exhibit the same behavior.

The system (51) - (59) is a closed system that will be used in the following to determine the evolution of the host system for given external pressure P and external Li flux $J_0(\tau)$.

5 Simulations

In this section we numerically study the proposed model (51) - (59). To this end we choose the following parameters as fixed:

The considered processes run at constant temperature $T_0 = 293.2$K and constant pressure $\bar{p} = 1$bar, i.e. $P = 0$. The atomic masses of Li and the matrix particles $FePO_4$ are $m_{\rm Li} = 3$ and $m_{\rm M} = 105$. The density of matrix particles is $\bar{n}_{\rm M} = 8.396\ 10^{28}$particles/m^3. The mechanical parameters bulk modulus, surface tension and maximal volume change are chosen as $K = 7.5\ 10^{10}$N/m^2, $\gamma = 0.075$N/m and $\delta = 0.06$. The free energy contains the interaction energy $\Omega = 94.4\ 10^{-22}$J/atom and the 3 parameters $a_0 = kT_0/\Omega = 0.390$, $a_1 = K/(\bar{n}_{\rm M}\Omega) = 11.5$ and $a_2 = \bar{p}/(\bar{n}_{\rm M}\Omega) = 0.000115$. Here $k = 1.38\ 10^{-23}$J/K denotes the Boltzmann constant. We choose the time and length scale of the model by $t_0 = 125664$s and $\bar{r}_0 = 20\ 10^{-9}$m, which is

the time scale of the external flux, respectively the radius of the host system for Li fraction $y = 0$.

The two relaxation times τ_{Li} and τ_{V} of the model are not known because they did not yet appear in the literature. However, we shall assume that they have values on a time scale which is much smaller than the time scale of the external flux, and in Section 5.3 we will give a short discussion on the influence of the choices of τ_{Li} and τ_{V} to the evolution of the host system.

5.1 Chemical Potentials

At first we discuss some properties of the chemical potentials $\mu \equiv \mu_{\mathrm{Li}} - \mu_{\mathrm{V}}$ and μ_{V}. Figures 4 and 5 show the both potentials without and with mechanical contributions. The mechanical phenomena are due to surface tension and Li induced volume changes of the matrix lattice. If these are ignored we were to have $\mu = f'(y)$ and $\mu_{\mathrm{V}} = f(y) - yf'(y)$ with f given by $(31)_2$. In this case the chemical potentials exclusively depend on the Li fraction y, which is represented by the red respectively green curve of Figure 4.

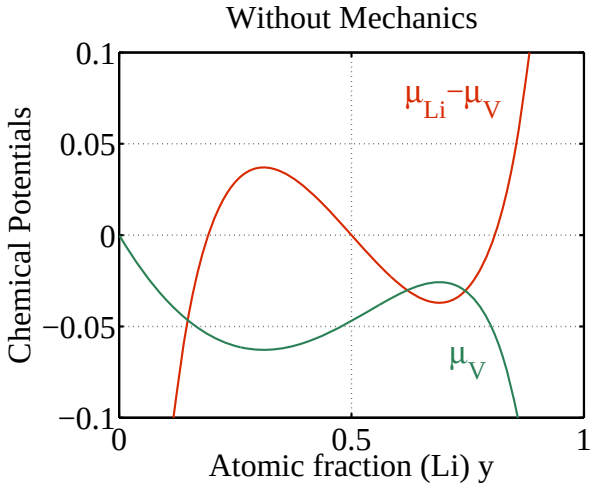

Figure 4: Relevant chemical potentials $\mu = \mu_{\mathrm{Li}} - \mu_{\mathrm{V}}$ and μ_{V} without mechanical contributions

If the mechanical phenomena are taken into account, the chemical potentials additionally depend on the location of the interface, i.e. on ξ_{I}. This dependence is illustrated in Figure 5 by the blue and green curves, which give the chemical potentials μ and μ_{V} for two different locations of the interface, viz. $\xi_{\mathrm{I}} = 0.43$ and $\xi_{\mathrm{I}} = 0.10$.

The difference $\mu = \mu_{\mathrm{Li}} - \mu_{\mathrm{V}}$ is not very much influenced by the location of the interface. This fact is important to understand the observed evolution of the voltage, which is determined by μ. On the other hand, the chemical potential of the vacancies

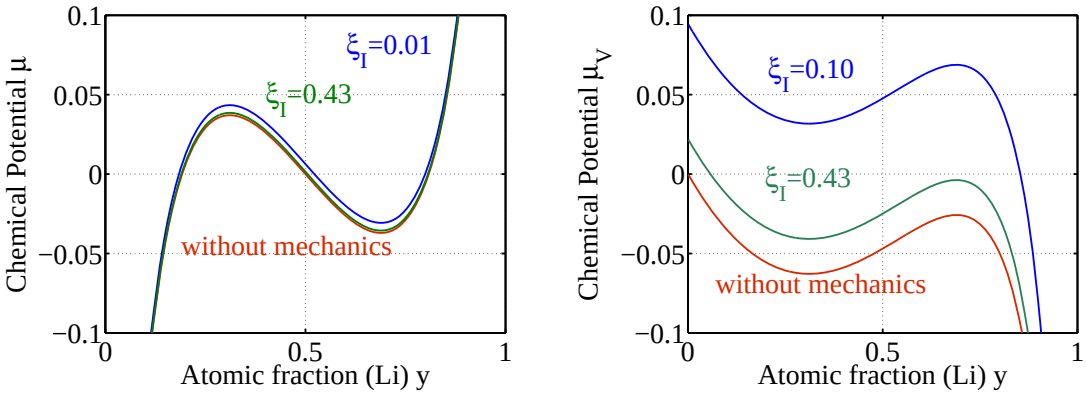

Figure 5: Red: Chemical Potentials as in Figure 4 without mechanical contributions. Blue and green: Chemical potentials with mechanical contributions for 2 different interfacial radii.

μ_{V} depends quite sensitive on a variation of ξ_{I}. This fact is related to the origin of the hysteretic behavior of the charging/discharging process of the battery.

Finally we discuss the non-monotonicity of the chemical potentials. It is sufficient to consider the difference μ. Let the Li fractions $y_1 < y_2$ indicate the boundaries of the two regions $0 \leq y < y_1$ and $y_2 < y \leq 1$ where μ is uniquely invertible with respect to y. If the total Li fraction q lies in either one of those ranges the Li distribution of the host system is represented by a single phase. For $y_1 \leq q \leq y_2$, there are three Li fractions corresponding to a given value of μ and the host system may decompose into two phases which are separated by an interface. The explicit determination of the region where the Li distribution is represented by two adjacent phases is a subtle problem that will be solved in the next sections of this study.

5.2 Possible equilibria

In this section we determine the possible equilibria for given q, i.e. total fraction q of stored Li atoms.

The conditions for possible equilibria consists of the two equations (24), which guarantee zero interfacial entropy production,

$$\mu^+(P, y^+) = \mu^-(P, \xi_{\mathrm{I}}, y^-) \quad \text{and} \quad \mu_{\mathrm{V}}^+(P, y^+) = \mu_{\mathrm{V}}^-(P, \xi_{\mathrm{I}}, y^-), \tag{60}$$

and of the Stefan condition (53)

$$y^+ = \frac{q - y^- \nu^-(P, \xi_{\mathrm{I}}, y^-)\xi_{\mathrm{I}}^3}{1 - \nu^-(P, \xi_{\mathrm{I}}, y^-)\xi_{\mathrm{I}}^3} \quad \text{with} \quad q = \frac{N_{\mathrm{Li}}}{N_{\mathrm{M}}}. \tag{61}$$

At first it is instructive to ignore the mechanical contributions. In that case, according to (58) and (59), the equations (60) reduce to the classical common tangent

construction

$$f'(y^+) = f'(y^-) \quad \text{and} \quad f(y^+) - y^+ f'(y^+) = f(y^-) - y^- f'(y^-), \tag{62}$$

which determine the so called Maxwell line. Up to a symmetry transformation the solution (y^+, y^-) of (62), which is indicated in Figure 6 by the two black dots, is unique. The symmetry of (62) implies that we may have $y^+ > y^-$ as well as $y^+ < y^-$. Furthermore it is important to note that a variation of the location of the interface does not change the equilibrium. After (62) is solved for (y^+, y^-) we may use the equation (61) in the form $q = (1 - \xi_{\mathrm{I}}^3)y^+ + \xi_{\mathrm{I}}^3 y^-$ to determine either the interface radius ξ_{I} or q, which gives the ratio of total number of Li atoms and total number of interstitial lattice sites.

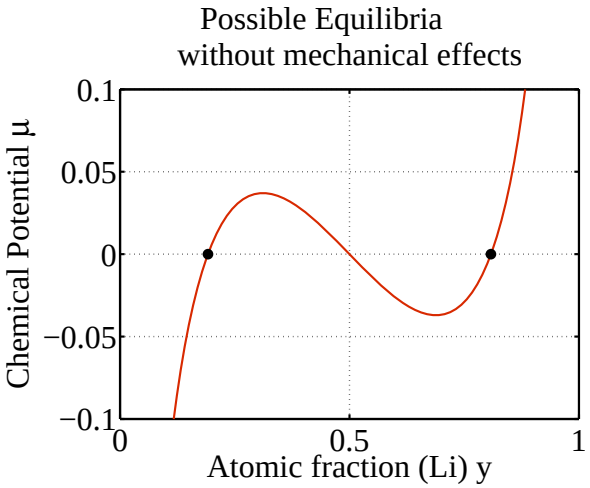

Figure 6: $\mu = \mu_{\mathrm{Li}} - \mu_{\mathrm{V}}$ and the two equilibria y^+ and y^- without mechanical contributions.

Next we include the mechanical phenomena into the discussion of the system (60), (61). In that case the radius ξ_{I} of the interface appears in (60), and thus the equilibria (y^+, y^-) depend on ξ_{I}.

There are two different compact domains of radii so that the triple $(y^+, y^-, \xi_{\mathrm{I}})$ solves the equations (60), and (61) serves to calculate the corresponding prescribed total Li fraction q. The first domain contains the radii for which we have $y^+ > y^-$, while in the second domain $y^+ < y^-$. There is no symmetry anymore between the outer and inner region of the host system. From the left plot of Figure 7 we may read off the possible atomic Li fractions in equilibrium, which are indicated by dots with blue color for $y^+ > y^-$, and with red color for $y^+ < y^-$.

The plot on the right hand side gives the corresponding interfacial radii for given total atomic Li fractions. It is important to note that for given q there is a region where two equilibria are possible.

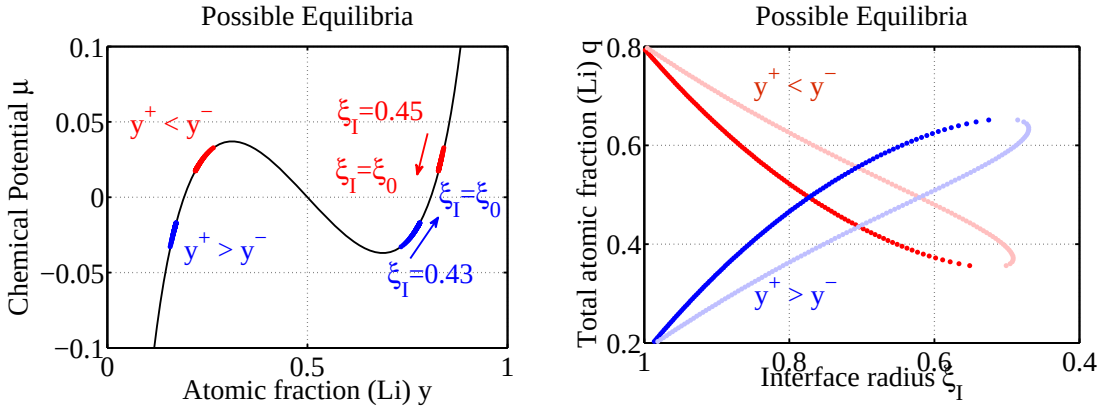

Figure 7: Possible equilibria when mechanical contributions are taken into account. Left: $\mu = \mu_{\mathrm{Li}} - \mu_{\mathrm{V}}$ and possible equilibria (y^+, y^-) for $y^+ > y^-$ (blue) and for $y^+ < y^-$ (red). Right : The corresponding interfacial radii ξ_{I} in equilibrium (dark colors). The points in light colors are energetical saddel points which also fulfill the necessary condition for equilibrium.

5.3 On the origin of the hysteretic behavior

Recall our assumption that during charging as well discharging the interface starts to appear at the outer radius with $y^+ < y^-$ during charging respectively with $y^+ > y^-$ during discharging.

We assume that the storage system approaches interfacial equilibrium on a much faster time scale than the loading respectively the unloading process. This assumption exhibits a hysteretic behavior of loading and unloading of the storage system.

For a demonstration of this statement we use the data from Figure 7 and the equation (58) to establish a plot that gives the chemical potential $-\mu^+ = -(\mu^+_{\mathrm{Li}} - \mu^+_{\mathrm{V}})$ versus the total electric charge of the cell shown in Figure 2, which is related to the total Li content of the host system by $1 - q$. If the electrolyte is treated as a liquid with infinite conductivity and if the anode consists of metallic Li, it can be shown that the voltage U of the lithium cell is given by $U = -(\mu^+_{\mathrm{Li}} - \mu^+_{\mathrm{V}})/e + \mathrm{const.}$.

We now compare the calculated hysteresis plot of Figure 8 with the corresponding experimental data from Figure 2 and observe that the orientation of the two hysteresis loops are opposite to each other.

Various reasons for this fundamental discrepancy are possible. In the current paper the exploitation of the model relies on several simplifying assumptions, viz. (i) only one $FePO_4$ particle of the cathode is modelled, (ii) fast bulk diffusion in comparison with the interface evolution, (iii) the shape of the interface is a sphere and (iv) the hysteresis is generated via local equilibrium states.

In [6] we derive and exploit a phase field model, whose sharp interface limit gives a special case of the model equations of this paper. Its numerical simulation shows that

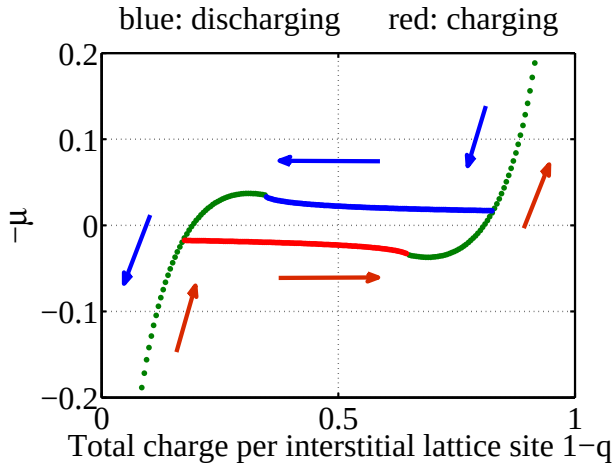

Figure 8: Equilibria states during charging and discharging. Regime of two coexisting phases: blue (discharging), red (charging). Single phase regime: green.

for fast loading, where diffusion in the bulk is the dominant process, the orientation of the hysteresis is reversed.

This is in accordance to the experimental orientation of Figure 2. However, the experimental charging rate is $C/10$, which is much slower than the time scale of diffusion, which is 4 s for $D \approx 10^{-16}$ m^2/s, [11], and a particle radius $r_0 \approx 20$ nm. Thus the phase field model of a single storage particle can not explain the outcome of the experiment.

In [7, 5] we explain the origin of the hysteresis in case of slow charging rate. We show that it is essential to consider the cathode as a system of many storage particles.

The determination of the regime where the phase transition within a single particle is the dominant process is still under discussion.

5.4 Evolutions for various initial and boundary data

In this section we discuss the behavior of the ODE system (51)-(52) for various q. The basic variables are the Li fraction y^- in the inner region Ω_-, and the interface radius ξ_{I}. All other system properties depend on these two variables, or are given constants.

Here we consider a constant $q = N_{\mathrm{Li}}/N_{\mathrm{M}}$, i.e. the total content of Li atoms in the storage system is constant during the evolution. In order to examine the evolutionary behavior of the ODE system (51)-(52) we examine the phase portrait. At first we discuss Figure 9, where we study $\mathrm{d}\xi_I/\mathrm{d}t$ isolines (left) and $\mathrm{d}y^-/\mathrm{d}t$ isolines (right) for $q = 0.5$ and $\tau_{\mathrm{Li}} = \tau_{\mathrm{M}} = 1$.

We note that the change of the Li fraction is of one order higher than the interfacial speed $\mathrm{d}\xi_I/\mathrm{d}t$ so that at first the interfacial Li fraction settles to an equilibrium, i.e.

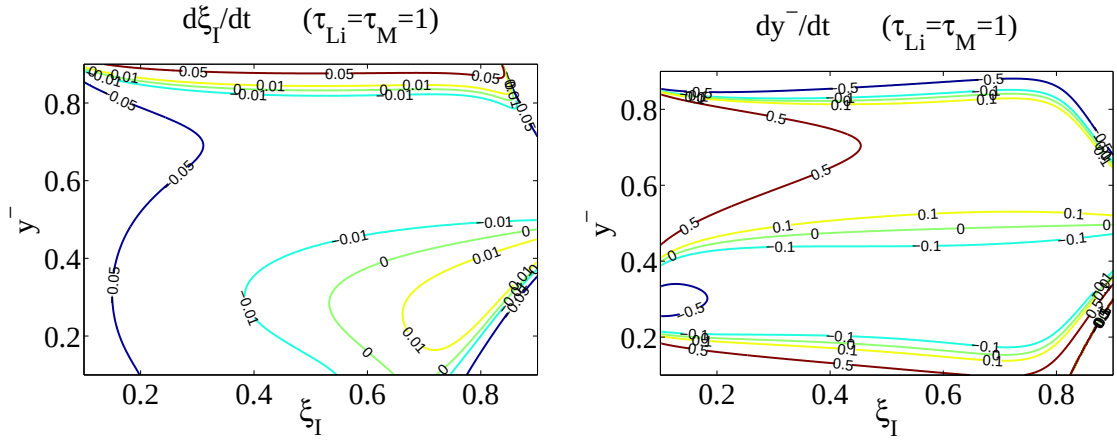

Figure 9: Visualization of phase portrait and domination of $\frac{\mathrm{d}y^-}{\mathrm{d}t}$

this is a state where $\mathrm{d}y^-/\mathrm{d}t = 0$. Hereafter the system evolves until the interface either reaches an equilibrium or it disappears, i.e. $\xi_I \to 0$ or resp. $\xi_I \to \xi_0$.

For the further discussion we write the ODE system (51)-(52) in a generic form and introduce the Jacobian J of the vector field F:

$$\begin{pmatrix} \mathrm{d}\xi_I/\mathrm{d}t \\ \mathrm{d}y^-/\mathrm{d}t \end{pmatrix} = \begin{pmatrix} F_1(\xi_I, y^-) \\ F_2(\xi_I, y^-) \end{pmatrix} \quad \text{and} \quad J(\xi_I, y^-) = \begin{pmatrix} \frac{\partial F_1}{\partial \xi_I} & \frac{\partial F_1}{\partial y^-} \\ \frac{\partial F_2}{\partial \xi_I} & \frac{\partial F_2}{\partial y^-} \end{pmatrix} . \tag{63}$$

In this context an equilibrium is an asymptotical stable point of rest of the ODE. To this end it is necessary that the two isolines $\mathrm{d}\xi_I/\mathrm{d}t = 0$ and $\mathrm{d}y^-/\mathrm{d}t = 0$ must cross, see Figure 10(a). However such an intersection is in general only known to be a point of rest for the ODE but must not be asymptotically stable. Further stability analysis distinguishes an asymptotical stable point of rest from an unstable one: $F(\xi_I, y^-) = 0$ is the condition for a point of rest, and if furthermore the eigenvalues of $J(\xi_I, y^-)$ have negative real parts, the point of rest is asymptotically stable.

We proceed with the examination of Figure 10, which contains isolines $\mathrm{d}\xi_I/\mathrm{d}t = 0$ and $\mathrm{d}y^-/\mathrm{d}t = 0$. Due to the dominance of $\mathrm{d}y^-/\mathrm{d}t$ almost everywhere, the vector field F is only visualized at two selected points by a horizontal arrow pointing left or right for $sign(\mathrm{d}\xi_I/\mathrm{d}t) = \pm 1$, and a vertical arrow for $\mathrm{d}y^-/\mathrm{d}t$ respectively.

The directions of the arrows change their sign at the corresponding isolines $\mathrm{d}\xi_I/\mathrm{d}t = 0$ and $\mathrm{d}y^-/\mathrm{d}t = 0$, and thus one can reproduce the qualitative behavior of the field $F(\xi_I, y^-)$ in every point. In order to give an impression to the overall behavior of the system, we also indicate the ratio of the interface speed $\mathrm{d}\xi_I/\mathrm{d}t$ and the change of Li fraction $\mathrm{d}y^-/\mathrm{d}t$ at those two selected points.

We are interested in the area where $0 \leq y^+(y^-, \xi_I),\ y^- \leq 1$ and $0 \leq \xi_I \leq \xi_0(y^-, \xi_I)$. The non physical area is roughly shaded. A special point of interest is where the particle is single phase. Such a state can be realized by an inner radius of $\xi_I = 0$, $y^+ = q$ and y^- arbitrary. Furthermore there is the point A, depicted in Figure 10(a), which represents $\xi_\mathrm{I} = \xi_0$,$y^- = q$ and y^+ arbitrary. Recall that the ODE system

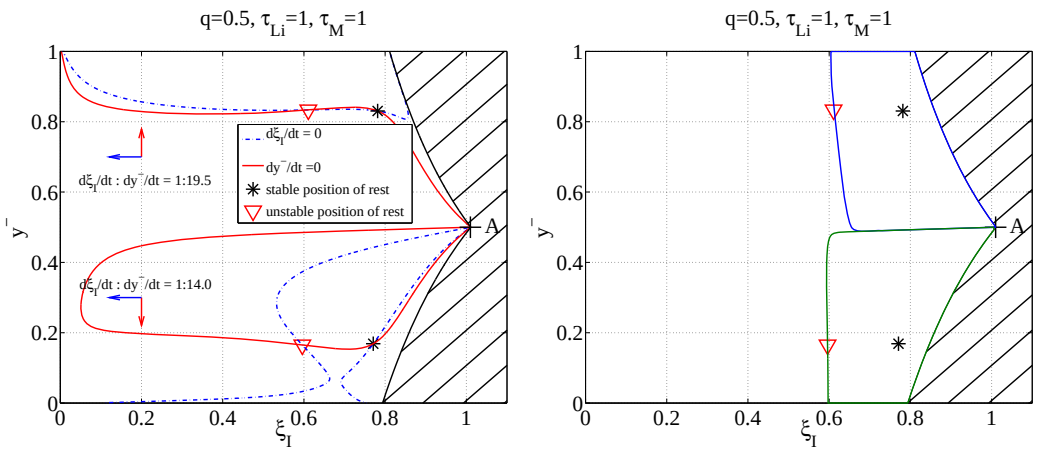

(a) isolines of zero horizontal or vertical flow (b) basin of attraction for positions of rest

Figure 10: Visualization of phase portrait

at hand describes a two phase system and the set $S := \{(y^-, \xi_I) \in [0,1] \times 0\} \cup A$ embodies single phase states. Thus the ODE system is not defined on S and these states can only be considered in the sense of limiting states.

Inspecting the asymptotic behavior of the ODE system reveals, that taking an arbitrary point in the physical region as starting point for the ODE, only three different results can occur in the asymptotical limit. The system ends either with a single phase ($\xi_I = 0$) or in one of the two stable points of rest, as depicted in Figure 10(a). To be precise, the system can theoretically also rest in asymptotical unstable point of rest. Such unstable point can even have an domain of attraction. However, since an arbitrary small disturbance of an unstable state drives the system into a stable point of rest or to a single phase state. From now on we ignore this possibility.

The basins of attraction for the two asymptotical stable points of rest are given in Figure 10(b). The whole region left of the two basins have the single phase with $\xi_I = 0$ as asymptotical limit. Each initial point in the vicinity of A, except A itself, lies in in one of the basins of attraction.

This supports the assumption that phase separation in the particle starts at the outer boundary of the storage particle during loading or unloading.

We now consider a loading rate $\dot{q}$ which is small compared to the time that is needed to approach equilibrium, i.e. we assume, that the dynamics of the ODE follows asymptotically stable points.

Thus we discuss now the quasi static behavior of the system by studying phase portraits for changing loading state q. For $q = 0.66$ and $q = 0.7$ these are given in Figures 11 and 12, which concern a situation where the equilibrium with low Li fraction vanishes.

In other words, a small variation of q implies a slight change of the stable points in Figure 11. However, there is a critical value q^* between 0.66 and 0.7, where the lower stable point disappears so that according to the field F, the system now moves

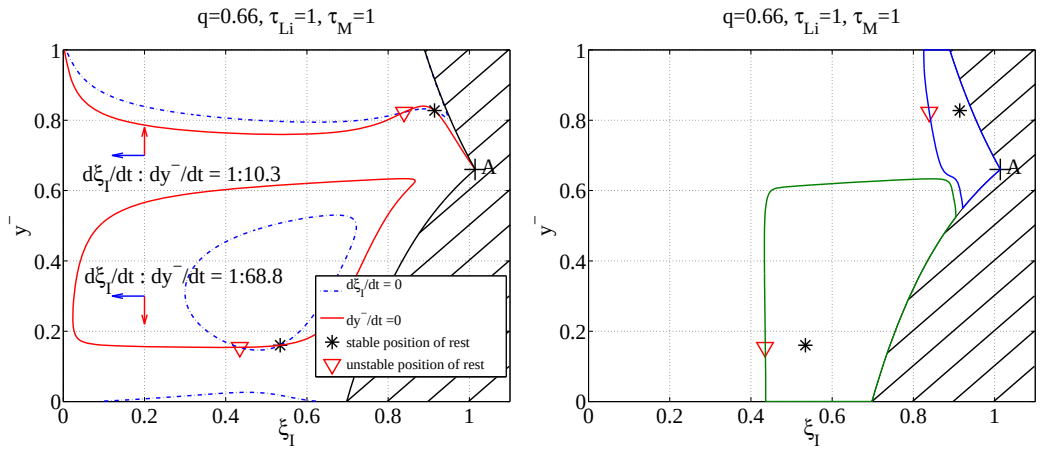

(a) isolines of zero horizontal or vertical flow (b) basin of attraction for positions of rest

Figure 11: Visualization of phase portrait for $\tau_{\mathrm{Li}} = \tau_{\mathrm{M}} = 1, q = 0.66$

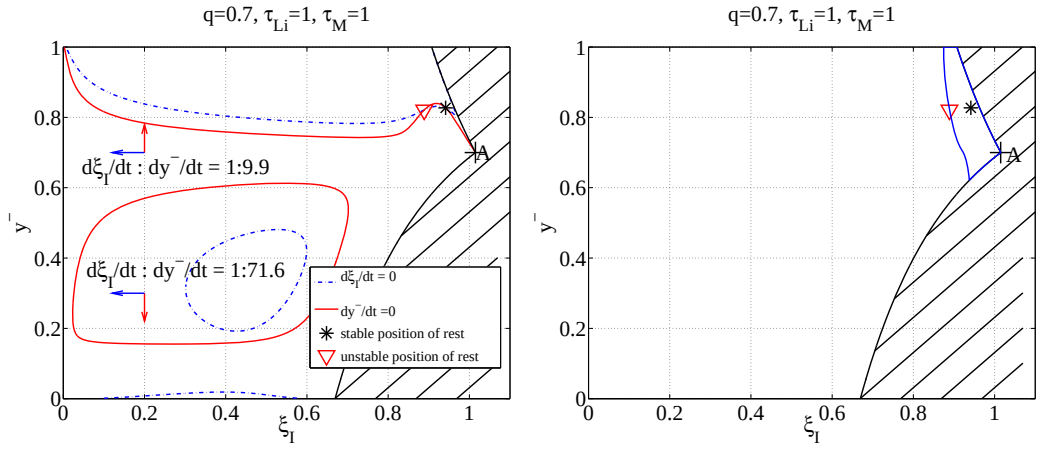

(a) isolines of zero horizontal or vertical flow (b) basin of attraction for positions of rest

Figure 12: Visualization of phase portrait for $\tau_{\mathrm{Li}} = \tau_{\mathrm{M}} = 1, q = 0.7$

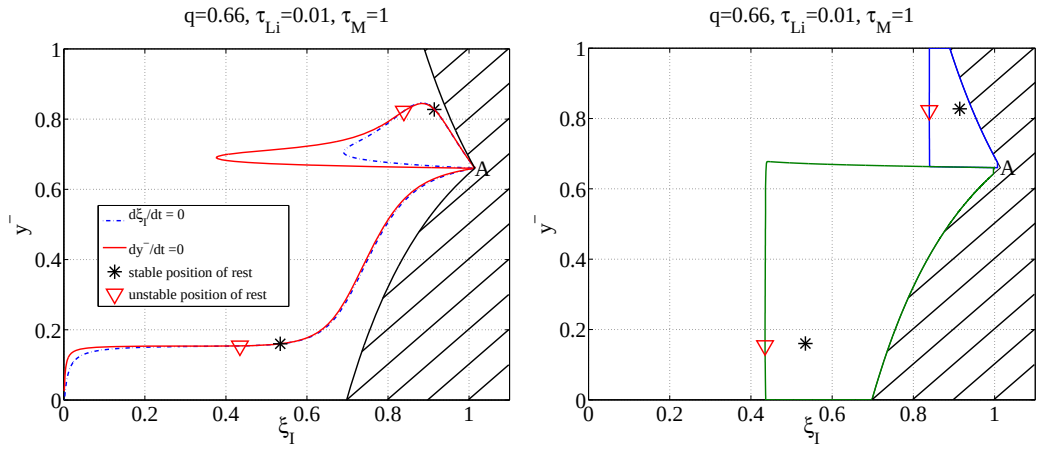

(a) isolines of zero horizontal or vertical flow (b) basin of attraction for positions of rest

Figure 13: Visualization of phase portrait for $\tau_{\mathrm{Li}} = 0.01, \tau_{\mathrm{M}} = 1, q = 0.66$

to $\xi_{\mathrm{I}} = 0$ describing a single phase state, see Figure 12.

The Figures 11 and 13 show the effect of changing the mobilities τ_{Li} and τ_{M} on the basins of attractions. For $\tau_{\mathrm{Li}} = 0.01$ and $\tau_{\mathrm{M}} = 1$ we observe in contrast to to the former case $\tau_{\mathrm{Li}} = 1$ and $\tau_{\mathrm{M}} = 1$ that points close to the single phase state A can now reach both asymptotically stable points of rest. Note that independent of the choice of mobilities, the points of rest of the ODE (51)-(52) stay the same. Likewise, the stable state of an inner core with low lithium fraction also vanishes, as q increases over the same threshold value q^* as before, for other choices of the interface mobilities, see Figure 13.

Conclusion

The model justifies the assumption, that phase separation sets in at the outer boundary. In other words, a second phase is likely to be developed at the outer boundary in form of a growing small outer shell.

In the model of the quasi static loading two different 2-phase configurations are possible as long as the loading state is between two thresholds $q \in (q_*, q^*)$. The stable 2-phase equilibria $(y_1^-(q), \xi_{I,1}(q))$ and $(y_2^-(q), \xi_{I,2}(q))$ differ by a higher $(y^- > y^+)$ or resp. lower $(y^- < y^+)$ Li fraction in the inner core.

We now consider a loading state $q \in (q_*, q^*)$ and stable configuration $(y_1^-(q), \xi_{I,1}(q))$, which moves continuously with q. For all loading states $\hat{q}$ close to q we know that $(y_1^-(q), \xi_{I,1}(q))$ must be in the basin of attraction of the stable point of rest $(y_1^-(\hat{q}), \xi_{I,1}(\hat{q}))$, considering the phase portrait belonging to $\hat{q}$. Thus the quasi static model does not allow a change from an inner core with high lithium fraction to an inner core with low fraction (or vice versa) in the two phase region $q \in (q_*, q^*)$.

However, there is a crucial experiment where such an change between different equilibria is observed for quasi-static loading. In [5] we describe the experiment in detail and show that a many particle storage system is needed to predict its outcome.

6 Appendix: Detailed description of motion, strain, stress and their influence on the chemical potentials

Introduction. In the current study we have described the deformation of the host system due to surface tension and Li induced volume changes of the crystal lattice within a simplified mechanical setting. In fact we have ignored that the host lattice of the $\mathrm{Li}_y\mathrm{FePO}_4$ particles have orthorhombic symmetry, so that 9 elastic constants are needed for a complete mechanical characterization. Furthermore we have ignored the deviatoric components of the stress, i.e. we have assumed the form $\sigma^{ij} = -p\delta^{ij}$.

In this section we shall give the necessary mechanical framework, i.e. we extend the

constitutive theory of Sections 3.1 - 3.4. The application to the case at hand will be done in a forthcoming paper. For those readers who are interested in more details concerning the following statements we refer to [2] and [3]. The determination of the elastic constants of $\mathrm{Li}_y\mathrm{FePO}_4$ and of the volume change due to lithiation is found to be in the recent study by Maxisch and Ceder [12].

Motion, strain and stress. At first we introduce a reference state in order to measure the motion of a material point of the $\mathrm{Li}_y\mathrm{FePO}_4$ matrix. Let $X = (X^i)_{i=1,2,3} = (X^1, X^2, X^3)$ be the location of a material point in a reference state, whose location at time t is given by $x = (x^i)_{i=1,2,3} = (x^1, x^2, x^3)$. The location x is determined by the function

$$x = \chi(t, X) = \big(\chi^1(t, X), \chi^2(t, X), \chi^3(t, X)\big). \tag{64}$$

We call $\chi(t, X) = (\chi^i(t, X))_{i=1,2,3}$ the motion of the material points of the crystal, and the displacement of a material point at X is denoted by

$$U^i(t, X) = \chi^i(t, X) - X^i. \tag{65}$$

The motion can be used to calculate the velocity, $\hat{v} = (\hat{v}^i)_{i=1,2,3}$, and the deformation gradient, $F = (F^{ij})_{i,j=1,2,3}$, of the crystal:

$$\hat{v}^i(t, X) = \frac{\partial \chi^i(t, X)}{\partial t}, \qquad F^{ij} = \frac{\partial \chi^i}{\partial X^j}. \tag{66}$$

We denote the Jacobian of F^{ij} by J, and we assume that $J > 0$, so that we may invert the motion $x^i = \chi^i(t, X)$ at any time t with respect to the coordinates X^i. We write

$$X^i = (\chi^{-1})^i(t, x), \tag{67}$$

and define the displacement field u^i by

$$u^i(t, x) = U^i(t, \chi^{-1}(t, x)). \tag{68}$$

This is a typical example for the representation of mechanical quantities with respect to actual coordinates. We call this representation the Euler or the spatial description, whereas the representation with respect to the reference coordinates is called the Lagrange or material description.

The velocity $\hat{v}^i(t, X)$ can likewise be given with respect to the coordinates x^i. We define $v^i(t, x) \equiv \hat{v}^i(t, \chi^{-1}(t, x))$, and we identify this quantity with the barycentric velocity that was introduced by $(9)_2$ in Section 3.1.

A similar definition for the mass density of the $\mathrm{Li}_y\mathrm{FePO}_4$ particles, viz. $\rho(t, x) = \hat{\rho}(t, \chi^{-1}(t, x))$, is useful to integrate the mass balance $(10)_1$ to obtain

$$J = \det(F) = \frac{\bar{\rho}}{\rho}, \tag{69}$$

where $\bar{\rho}$ is the mass density for $F^{ij} = \delta^{ij}$.

Further important objects for the description of the stretch are the right and the left Cauchy-Green tensor, C^{ij} and B^{ij}, and for the description of the strain we define the Green strain tensor G^{ij}:

$$C^{ij} = F^{mi}F^{mj}, \quad B^{ij} = F^{im}F^{jm}, \quad G^{ij} = \frac{1}{2}(C^{ij} - \delta^{ij}). \tag{70}$$

These quantities may also easily be given with respect to the spatial representation.

Next we decompose the stretch of a body into a part, which gives pure volume changes of the body and the complementary part, which describes pure changes of its shape. Pure changes of the volume are obviously given by the Jacobian J, whereas the unimodular tensor

$$c^{ij} \equiv J^{-2/3}C^{ij} \quad \text{with} \quad \det(\boldsymbol{c}) = 1 \tag{71}$$

represents changes of the shape of a body.

Furthermore we need to introduce two measures of stress: (i) the Cauchy stress $\sigma^{ij} = \sigma^{ji}$, which gives the actual force per actual surface element and (ii) the second Piola-Kirchhoff stress t^{ik}, which is defined by

$$t^{ij} = J(F^{-1})^{im}(F^{-1})^{jn}\sigma^{mn}. \tag{72}$$

The isotropic part of the Cauchy stress is related to the pressure p, which is defined by

$$p = -\frac{1}{3}\sigma^{mm}, \quad \text{so that} \quad \sigma^{ij} = -p\,\delta^{ij} + \sigma^{\langle ij\rangle} \quad \text{with} \quad \sigma^{\langle jj\rangle} = 0. \tag{73}$$

Here the angle brackets indicate the stress deviator, which represents the stress due to pure changes of the shape of a solid, whereas the pressure is related to pure changes of its volume.

Free energy, chemical potentials and stress. In the simplified mechanical treatment, the specific free energy relies on the representation (17): $\psi = \hat{\psi}(T, n_{\mathrm{Li}}, n_{\mathrm{V}}) = \tilde{\psi}(T, y, \rho)$. Its generalization to the complete mechanical description reads

$$\psi = \hat{\psi}(T, n_{\mathrm{Li}}, n_{\mathrm{V}}, c^{ij}) = \tilde{\psi}(T, y, \rho, c^{ij}) = \check{\psi}(T, y, C^{ij}). \tag{74}$$

The calculation of the chemical potentials and the pressure, which is now defined by $p = -\sigma^{nn}/3$, rely on the same rules as before, i.e. according to (19) we have

$$\mu_{\mathrm{Li}} = \frac{\partial\rho\hat{\psi}}{\partial n_{\mathrm{Li}}}, \quad \mu_{\mathrm{V}} = \frac{\partial\rho\hat{\psi}}{\partial n_{\mathrm{V}}}, \quad p = \rho^2\frac{\partial\tilde{\psi}}{\partial\rho}, \quad \rho\psi + p = \mu_{\mathrm{Li}}n_{\mathrm{Li}} + \mu_{\mathrm{V}}n_{\mathrm{V}}, \tag{75}$$

and the function $\check{\psi}(T, y, C^{ij})$ is used to calculate the 2$^{\mathrm{nd}}$ Piola Kirchhoff stress by means of

$$t^{ij} = 2\bar{\rho}\frac{\partial\check{\psi}}{\partial C^{ij}}. \tag{76}$$

Interfacial entropy inequality and kinetic relations. In order to obtain the interfacial entropy inequality for the complete mechanical description we have to

substitute in (22) $\sigma^{ij} = -p\delta^{ij} + \sigma^{<ij>}$ instead of $\sigma^{ij} = -p\delta^{ij}$. After some simple algebraic manipulations we now end up with

$$\dot{\mathcal{N}}_{\rm Li}[[\mu_{\rm Li}-\mu_{\rm V}-\frac{m_{\rm Li}}{\rho}\sigma^{<ij>}\nu^i\nu^j+\frac{m_{\rm Li}}{2}(v-w)^2]]+\dot{\mathcal{N}}_{\rm M}[[\mu_{\rm V}-\frac{m_{\rm M}}{\rho}\sigma^{<ij>}\nu^i\nu^j+\frac{m_{\rm M}}{2}(v-w)^2]] \geq 0. \tag{77}$$

The normal ν, with $\nu^i\nu^i = 1$, of the interface points into the + region. The velocity of the interface is w, and w^ν denotes its normal speed.

We observe that we may read off from (77) kinetic relations of the same formal structure as it is given by (25). The important difference to the case with pure pressure is the contribution of the jump of the stress deviator to the driving forces. Preliminary numerical calculations reveal that this contribution may induce that a spherical as well as a flat interface may become unstable.

Decomposition of total strain into elastic and misfit strain. This paragraph introduces the appearing peculiarities that we meet if we describe the deformation of a solid that consists of several constituents. The following discussion gives the basic prerequisite to formulate the appropriate constitutive law that relates the stress to the strain. We choose as variables the Li fraction and the deformation gradient, i.e. (y, F).

We consider a reference state $\bar{S}$ with $(\bar{y} = 0, \bar{F}^{ij} = \delta^{ij})$, an intermediate state S_* with $(y_* = y, F_*^{ij})$ and the actual state S with (y, F^{ij}). We assume, that these states are related to each other by the following conditions: (i) The intermediate state is reached from the reference state under constant reference stress $\sigma^{ij} = -\bar{p}\delta^{ij}$. (ii) The transition of the intermediate state to the actual state by F_e^{ij} at constant Li fraction y leads to elastic stress $\sigma^{ij} \neq -\bar{p}\delta^{ij}$. For this reason we call F_e^{ij} the elastic part of the deformation gradient.

By means of the given rules we have decomposed the change of the state of a solid into two parts, without and with deviations from the hydrostatic reference stress. The deformation gradient F_*^{ij} might be due to thermal expansion, which we do not consider here, or/and due to the change of shape and volume because we have a change of the Li fraction from $\bar{y} = 0$ to $y_* = y$. In any case, F_*^{ij} is experimentally measured at the reference stress. On the other hand, elastic stresses are exclusively due to changes of the atomic distances of the crystal lattice at fixed occupation of lattice sites.

The reference, the intermediate and the actual state have mass densities $\bar{\rho}$, ρ_*, ρ, particle densities $\bar{n}_{\rm M}$, $n_{\rm M}^*$ $n_{\rm M}$ and Li fractions $\bar{y} = 0$, $y_* = y$, y. We thus have

$$\bar{\rho} = m(\bar{y})\bar{n}_{\rm M}, \quad \rho_* = m(y)n_{\rm M}^*, \quad \text{and} \quad \rho = m(y)n_{\rm M}, \tag{78}$$

so that the three Jacobians $J_* = \det(F_*) = \bar{\rho}/\rho_*$, $J_e = \det(F_e) = \rho_*/\rho$ and $J = \det(F) = \bar{\rho}/\rho$ are given by

$$J_* = \nu(y)\frac{\bar{n}_{\rm M}}{n_{\rm M}^*}, \quad J_e = \frac{n_{\rm M}^*}{n_{\rm M}}, \quad J = \nu(y)\frac{\bar{n}_{\rm M}}{n_{\rm M}} \quad \text{with} \quad \nu \equiv \frac{m(\bar{y})}{m(y)}. \tag{79}$$

There is a multiplicative decomposition of the total deformation gradient according to

$$F^{ij} = F_e^{ik} F_*^{kj}, \tag{80}$$

which results by a simple geometric reasoning: We have three motions: The total motion from $\bar{S}$ to S: $x^i = \chi^i(t, X)$, the motion at constant reference stress from $\bar{S}$ to S_*: $X_*^i = \chi_*^i(t, X)$ and the pure elastic motion from S_* to S: $x^i = \chi_e^i(t, X_*)$. The chain rule implies

$$F^{ij} = \frac{\partial \chi^i}{\partial X^j} = \frac{\partial \chi_e^i}{\partial X_*^k} \frac{\partial \chi_*^k}{\partial X^j} = F_e^{ik} F_*^{kj}. \tag{81}$$

The St.Venant-Kirchhoff law. We denote the 2nd Piola-Kirchhoff stresses with respect to the states $\bar{S}$ and S_* by t^{ij} and z^{ij}, respectively. Obviously the both stresses give the same (actual) Cauchy stress by

$$\sigma^{ij} = \frac{1}{J} F^{ik} F^{jl} t^{kl} \quad \text{and} \quad \sigma^{ij} = \frac{1}{J_e} F_e^{ik} F_e^{jl} z^{kl}, \tag{82}$$

and by elimination of σ^{kl} we obtain with (80)

$$t^{ij} = J_* F_*^{-ik} F_*^{-jl} z^{kl}. \tag{83}$$

Recall that the transformation from S_* to S is purely elastic, so that we have to formulate the elastic stress strain relation for z^{ij}. For small strains we may use the St. Venant-Kirchhoff law which reads

$$z^{ij} = -\bar{p} J_e C_e^{-ij} + \frac{1}{2} \tilde{K}^{ijkl}(y)(C_e^{kl} - \delta^{kl}). \tag{84}$$

$C_e^{ij} = F_e^{ki} F_e^{kj}$ is the elastic Cauchy-Green tensor. The stiffness matrix $\tilde{K}^{ijkl}(y)$ depends on the Li fraction and satisfies the general symmetries $\tilde{K}^{ijkl} = \tilde{K}^{jikl} = \tilde{K}^{ijlk} = \tilde{K}^{klij}$.

In order to obtain the free energy density according to (76) we have to calculate the stress-strain relation for the stress t^{ij}. We insert the elastic law (84) into (83) and define a stiffness matrix K^{ijkl} and a misfit strain C_*^{ij} by

$$K^{ijkl}(y) \equiv J_* F_*^{-im} F_*^{-jn} F_*^{-ko} F_*^{-lp} \tilde{K}^{mnop}(y) \quad \text{and} \quad C_*^{ij} \equiv F_*^{ki} F_*^{kj}. \tag{85}$$

After some algebraic manipulations we finally obtain

$$t^{ij} = -\bar{p} J C^{-ij} + \frac{1}{2} K^{ijkl}(y)(C^{kl} - C_*^{kl}(y)). \tag{86}$$

The experimental data given by Maxisch and Ceder, [12] can be used to calculate the various components of the stiffness matrix and the misfit strain. Unfortunately the authors do not indicate whether their measurements rely on the stress-strain relation (84) or on (86). However, we think they have used (84).

Free energy density and chemical potentials for the St.Venant-Kirchhoff law. The mechanical part of the free energy density relies on the thermodynamic relation (76). By simple integration and by including the chemical part we obtain

$$\rho\psi = n_{\mathrm{M}}\Omega f(y) + \bar{p}(\frac{J_*}{J} - 1) + \frac{1}{8J}(C^{kl} - C_*^{kl})K^{klnm}(C^{nm} - C_*^{nm}). \tag{87}$$

In order to calculate the chemical potentials according to $(75)_{1,2}$, we must represent $\rho\psi$ in the variables n_{Li}, n_{V} and c^{ij}, recall $c^{ij} = (\nu(y)\bar{n}_{\mathrm{M}}/n_{\mathrm{M}})^{-2/3}C^{ij}$. We obtain for lithium

$$\begin{aligned}\mu_{\mathrm{Li}} &= \Omega(f + (1-y)f')+ \\ &\frac{1}{\bar{n}_{\mathrm{M}}\nu}((\frac{m_{\mathrm{Li}}}{m_{\mathrm{M}}}\nu(1-y)+1)(\bar{p}J_* - \frac{1}{8}(\frac{1}{3}C^{kl} + C_*^{kl})K^{klmn}(C^{mn} - C_*^{mn}))+ \\ &(1-y)(\bar{p}J'_* + \frac{1}{8}(C^{kl} - C_*^{kl})K'^{\ klmn}(C^{mn} - C_*^{mn}) - \frac{1}{2}C'^{\ kl}_* K^{klmn}(C^{mn} - C_*^{mn}))),\end{aligned} \tag{88}$$

and for the vacancies

$$\begin{aligned}\mu_{\mathrm{V}} &= \Omega(f - yf')+ \\ &\frac{1}{\bar{n}_{\mathrm{M}}\nu}(-(\frac{m_{\mathrm{Li}}}{m_{\mathrm{M}}}\nu y - 1)(\bar{p}J_* - \frac{1}{8}(\frac{1}{3}C^{kl} + C_*^{kl})K^{klmn}(C^{mn} - C_*^{mn}))- \\ &y(\bar{p}J'_* + \frac{1}{8}(C^{kl} - C_*^{kl})K'^{\ klmn}(C^{mn} - C_*^{mn}) - \frac{1}{2}C'^{\ kl}_* K^{klmn}(C^{mn} - C_*^{mn}))),\end{aligned} \tag{89}$$

where a prime indicates the derivative with respect to the Li fraction y.

Thus we have completed the constitutive theory for the host system with chemical and mechanical coupling.

References

[1] J.L. Allen, T.R. Jow and J. Wolfenstine, *Kinetic Study of the Electrochemical $FePO_4$ to $LiFePO_4$ Phase transition*, Chemical Materials **19** (2004), 2108–2111.

[2] T. Böhme, W. Dreyer, F. Duderstadt, and W.H. Müller *A higher gradient theory of mixtures for multi-component materials*, WIAS Preprint No. 1286, Philosophical Magazine submitted (2007).

[3] W. Dreyer, *Jump Conditions at phase boundaries for ordered and disordered phases*, WIAS Preprint No. 869 (2003).

[4] W. Dreyer and F. Duderstadt, *On the modelling of semi-insulating GaAs including surface tension and bulk stresses*, WIAS Preprint No. 995, to appear in Proc. R. Soc. A (2008).

[5] W. Dreyer, M. Gaberšček, C. Guhlke, R. Huth and J. Jamnik, *The thermodynamic origin of hysteresis in insertion batteries*, in preparation (2009)

[6] W. Dreyer, C. Guhlke, *A phase field model and its sharp interface limit*, WIAS Preprint in preparation (2009)

[7] W. Dreyer, C. Guhlke and R. Huth, *The behavior of a many particle cathode in a lithium-ion battery*, WIAS Preprint No. 1423 (2009).

[8] M. Gaberšček, R. Dominko and J. Jamnik, *The meaning of impedance measurements of LiFePO4 cathodes: A linearity study*, J. power sources **174** (2007), 944-948.

[9] M. Gaberšček, R. Dominko, M. Bele, M. Remškar, D. Hanzel and J. Jamnik, *Porous, carbon-decorated LiFePO4 prepared by sol-gel method based on citric acid*, Solid State Ionics **176** (2005), 1801–1805.

[10] P.M. Gomadam and J.W. Weidner, *Modeling Volume Changes in Porous Electrodes*, Journal of The Electrochemical Society **153**(1) (2006), A179–A186.

[11] B.C. Han, A. Van der Ven, D. Morgan and G. Ceder, *Electrochemical modeling of intercalation processe with phase field models*, Electrochimica Acta **49** (2004), 4691–4699.

[12] T. Maxisch and G. Ceder, *Elastic properties of olivine Li_xFePO_4 from first principles*, Physical Reviev B**73** (2006), 174112-1–174112-4.

[13] V. Srinivasan and J. Newman, *Discharge Model for the Lithium Iron-Phosphate Electrode*, Journal of The Electrochemical Society **151**(10) (2004), A1517–A1529.

[14] M. Wagemaker, W.J.H. Borghols and F.M. Mulder, *Large Impact of Particle Size on Insertion Reaction. A Case for Anatase Li_xTiO_2*, J. AM. CHEM. SOC. **129**(14) (2007), 4323–4327.

[15] A. Yamada, H. Koizumi, S.I. Nishimura, N. Sonoyama, R. Kanno, M. Yonemura, T. Nakamura and Y. Kobayashi, *Room-temperature miscibility gap in Li_xFePO_4*, Nature materials Letters **5** (2006), 357–360.